Macromolecular Research, Vol. 12, No. 1, pp 1-10 (2004)

Macromolecular Research

Volume 12, Number 1 February 28, 2004

Feature Article

Structural Changes in Isothermal Crystallization Processes of Synthetic Polymers Studied by Time-Resolved Measurements of Synchrotron-Sourced X-Ray Scatterings and Vibrational Spectra

Kohji Tashiro* and Hisakatsu Hama

Department of Macromolecular Science, Graduate School of Science, Osaka University, Toyonaka, Osaka 560-0043, Japan

Received Aug. 28, 2002; Revised Dec. 2, 2002

Abstract: The structural changes occurring in the isothermal crystallization processes of polyethylene (PE), polyoxymethylene (POM), and vinylidene fluoridetrifluoroethylene (VDFTrFE) copolymer have been reviewed on the basis of our recent experimental data collected by the time-resolved measurements of synchrotron-sourced wide-angle (WAXS) and small-angle X-ray scatterings (SAXS) and infrared spectra. The temperature jump from the melt to a crystallization temperature could be measured at a cooling rate of 600-1,000 °C/min, during which we collected the WAXS, SAXS, and infrared spectral data successfully at time intervals of ca. 10 sec. In the case of PE, the infrared spectral data clarified the generation of chain segments of partially disordered trans conformations immediately after the jump. These segments then became transformed into more-regular all-trans-zigzag forms, followed by the formation of an orthorhombic crystal lattice. At this stage, the generation of a stacked lamellar structure having an 800-Å-long period was detected in the SAXS data. This structure was found to transfer successively to a more densely packed lamellar structure having a 400-Å-long period as a result of the secondary crystallization of the amorphous region in-between the original lamellae. As for POM, the formation process of a stacked lamellar structure was essentially the same as that mentioned above for PE, as evidenced from the analysis of SAXS and WAXS data. The observation of morphology-sensitive infrared bands revealed the evolution of fully extended helical chains after the generation of lamellae having folded chain structures. We speculate that these extended chains exist as taut tie chains passing continuously through the neighboring lamellae. In the isothermal crystallization of VDFTrFE copolymer from the melt, a paraelectric high-temperature phase was detected at first and then it transferred into the ferroelectric low-temperature phase at a later stage. By analyzing the reflection profile of the WAXS data, the structural ordering in the high-temperature phase and the ferroelectric phase transition to the low-temperature phase of the multi-domain structure were traced successfully.

Keywords: isothermal crystallization, synchrotron X-ray, infrared spectra, polyethylene, polyoxymethylene, vinylidene fluoride copolymer.

*e-mail: ktashiro@chem.sci.osaka-u.ac.jp
1598-5032/02/1-10©2004 Polymer Society of Korea

Introduction

When we try to trace the structural evolution in the crystallization process of synthetic polymers, we need to carry out the time-resolved measurements of various kinds of techniques such as X-ray scattering, infrared spectroscopy, Raman spectroscopy, small-angle light scattering, etc.[1] But, in most of papers, the data were collected by a single kind of methodology and therefore the interpretation was made only from one-sided point of view. In order to clarify the details of structural changes, however, we have to combine the different types of data together in an organized manner. For example a combination of the wide-angle (WAXS) and small-angle X-ray scattering (SAXS) techniques with the infrared/Raman spectroscopy is though to be quite useful for the clarification of the structural evolution processes from the microscopic point of view. The most ideal way is to carry out the simultaneous measurement of these various techniques for one sample, but this approach is still in progress.[1,2]

In this paper we will briefly review our recent experimental results obtained for several kinds of polymer and will extract some essential and common features in the crystallization behavior of these polymers. As examples, we will treat here the isothermal crystallization of polyethylene (PE), polyoxymethylene (POM), and vinylidene fluoride-trifluoroethylene (VDF-TrFE) copolymer. PE and POM are basically important polymers and their crystallization behaviors had been investigated by many researchers for a long time. But the microscopically-viewed structural changes have not yet been clarified enough well. VDF-TrFE copolymer is only one synthetic polymer exhibiting the so-called ferroelectric-to-paraelectric phase transition. When this copolymer is cooled from the melt, it is expected that the complicated structural changes may occur because both the crystallization and ferroelectric transition occurs in the cooling process. In the present paper the structural changes occurring in these crystallization and phase transition phenomena are described concretely from the levels of molecular chains and aggregation state of these chains.

Experimental

Samples. PE samples used in the isothermal crystallization experiment were high-density PE (M_w = 126 k, M_w/M_n = 5.3) and linear low-density PE (17 ethyl branch/1000 C, M_w = 75 k, M_w/M_n = 2.0) supplied by Exxon Chemicals Inc. The latter sample exhibits slower crystallization than high-density PE and was useful to collect the X-ray and infrared data from the earliest stage of without any loss of essential features of the crystallization behavior. In the crystallization study of POM, a copolymer of trioxane with small amount of ethylene oxide (ca. 2.2 wt%) was used, which was supplied by Polyplastics Co. Ltd., Japan (M_w = 69 k, M_w/M_n = 2.3), in order to avoid the easily-occurred thermal decomposition as much as possible without any loss of characteristic crystallization behavior of POM homopolymer. VDF-TrFE copolymer sample with VDF 73 mol% was supplied by Daikin Co. Ltd., Japan.

Temperature Jump and Time-Resolved Measurements. In the study of isothermal crystallization process, one of the most important procedures is to perform a rapid temperature jump from high temperature (T_1) to low temperature (T_2) and a stabilization of T_2 with as small fluctuation as possible. We developed the temperature jump cells for FTIR and WAXS/SAXS measurements with a jump rate of 600-1,000 °C/min and the temperature fluctuation less than 0.2 °C.[3] The temperature of the sample was measured directly by embedding a thermocouple into the sample.

Since the crystallization completes in a short time, we used a synchrotron radiation for the WAXS and SAXS measurements by coupling with a position-sensitive proportional detector. The time-resolved WAXS and SAXS measurements were performed in beam lines 15A and 10C of KEK (High-energy Accelerator Research Organization) in Tsukuba, Japan. The collection time was 3-7 sec for one shot at a time interval of 3-7 sec. For the rapid-scanning infrared spectral measurement, a Bio-Rad FTS-60A/896 FT-IR spectrometer with an MCT detector was used. The collection time of one spectrum was 1-4 sec at a resolution power of 2 cm^{-1}.

Results and Discussion

Isothermal Crystallization of Polyethylene. The crystallization of polyethylene (PE) occurs very quickly in a time scale of several minutes, although the crystallization rate depends on the degree of supercooling. In order to trace the chain conformational change during the crystallization process the time-resolved infrared measurement was made for the linear low-density PE sample.[4] This sample crystallizes at relatively lower rate than the case of high-density PE and was easier to investigate the structural evolution in details without any loss of essential features of crystallization behavior of high-density PE. Figure 1 shows the time dependence of integrated intensity estimated for the infrared bands characteristic of various types of chain conformation, where the infrared data were measured during the isothermal crystallization at the degree of supercooling (ΔT) of 4 °C. Immediately after the temperature jump from the molten state, the infrared bands characteristic of disordered trans conformation started to appear and increased in intensity. When the intensity of this band started to decrease, the infrared bands of all trans-zigzag conformation started to increase in intensity. At the same time the splitting of regular trans bands was detected, indicating a formation of orthorhombic crystal lattice. In parallel the SAXS measurement was carried out with a synchrotron radiation system.[5] By performing a Fourier-transformation of the SAXS intensity data after the correction of Lorenz-factor, the invariant, the long period of stacked

lamellae, the lamellar thickness, and so on were evaluated as shown in Figure 2. In the early stage of crystallization, the scattering intensity of the central peak was found to increase, suggesting an increase of density fluctuation in the molten sample. After that, the peak (L_1) corresponding to the lamellar stacking structure of 800 Å long period started to appear and increased in intensity (region II in Figure 2). As the time passed furthermore, the lamellar thickness increased and the long period changed to ca. 400 Å (L_2) due to the secondary crystallization of the amorphous region in between the initially-formed crystalline lamellae (region III in Figure 2). In Figure 3, where the WAXS data collected in the temperature jump experiments at $\Delta T = 1$ and 2 °C are

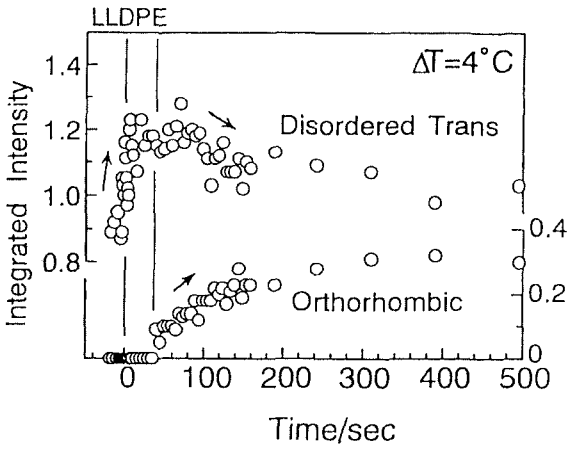

Figure 1. Time dependence of integrated intensity of infrared bands characteristic of conformationally-disordered-trans and regular trans forms evaluated for linear low-density PE in the isothermal crystallization process from the melt (quoted from K. Tashiro, S. Sasaki, N. Gose, and M. Kobayashi, *Polym. J.*, **6**, 485 (1998)).

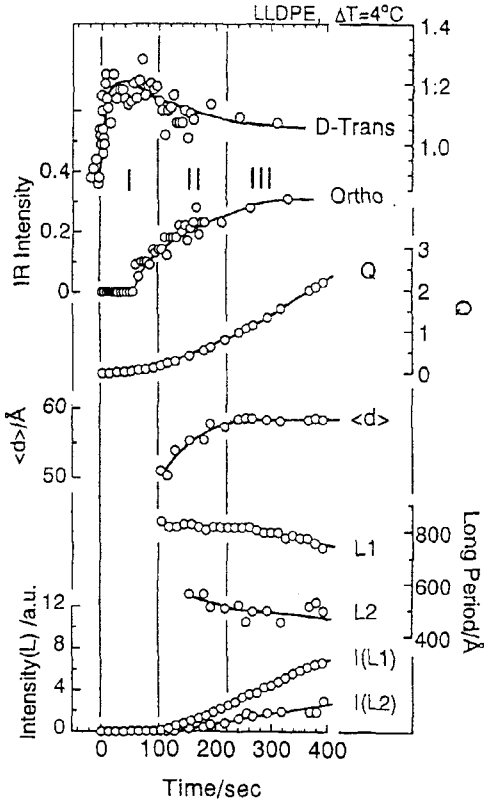

Figure 2. Comparison of the vibrational spectroscopic data with the SAXS data collected for linear low-density PE sample in the isothermal crystallization process from the melt. Q: invariant, $\langle d \rangle$: lamellar thickness, L_1 (800 Å) and L_2 (400 Å) denote, respectively, the long periods of the lamellar stacking structure. $I(L_1)$ and $I(L_2)$ denote the SAXS intensities measured for the correspon-ding peaks (quoted from S. Sasaki, K. Tashiro, M. Kobayashi, Y. Izumi, and K. Kobayashi, *Polymer*, **40**, 7125 (1999)).

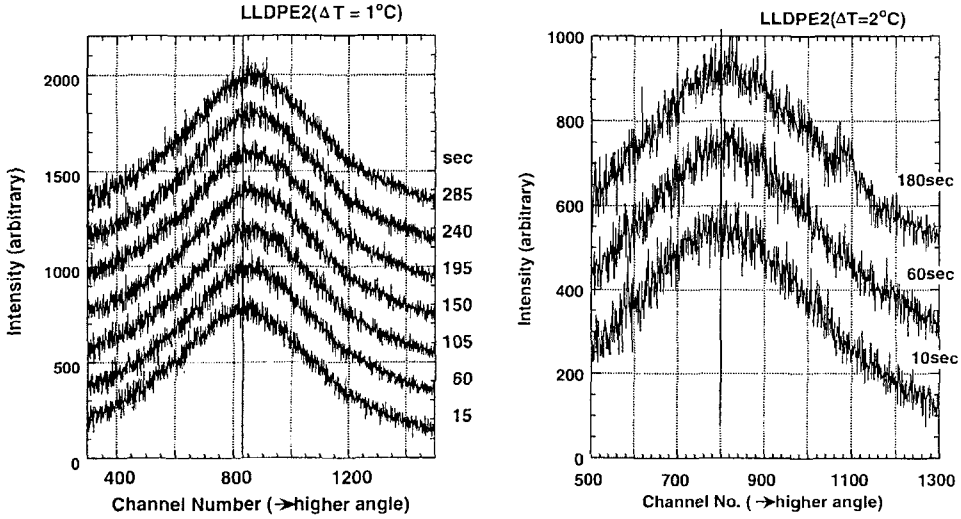

Figure 3. Time dependence of WAXS profiles measured in the isothermal crystallization process of linear low-density PE at $\Delta T = 1$ and 2 °C (quoted from K. Tashiro, *KEK Proceedings*, **2001-24**, 5 (2002)).

shown, the peak of the amorphous halo was found to shift to higher scattering angle side with a passage of time before the observation of crystalline reflections, suggesting that the amorphous phase is contracted gradually and then the nucleation of crystallites is started in the higher density regions of the density-fluctuating melt.[6]

By combining all of the above-mentioned experimental data, we may describe the crystallization process of orthorhombic polyethylene in the following way and as seen in Figure 4.[7] Immediately after the sample is cooled rapidly from the melt to the crystallization temperature, the density fluctuation occurs in the molten sample, as known from the increment of central peak intensity of SAXS profile, and the partially-disordered trans chain segments generate in the regions of higher density, as supported by the WAXS observation about the gradual contraction of the amorphous phase and also the observation of infrared bands of disordered trans conformation (time region I). In the time region II, these partially-disordered trans segments gather together and regularize into orthorhombic crystalline lattice consisting of planar-zigzag chain segments, being confirmed by the intensity increment of the infrared bands and WAXS reflections characteristic of orthorhombic crystal form. The thus-created lamellae are stacked at the long period of ca. 800 Å (L_1 in Figure 2). As the time passes furthermore, the secondary crystallization occurs in the amorphous parts sandwiched between these stacked lamellae to form new lamellae, resulting in the observation of SAXS peak of long period 400 Å (L_2 in Figure 2, time region III). In Figure 4 it is noted that the radius of gyration (R_g) of a chain is kept almost constant before and after the crystallization and the chain folding mode on the lamellar surfaces is essentially of random reentry type. These information were deduced from the experimental data of small- and wide-angle neutron scatterings, infrared spectra, and differential scanning calorimetry measured for a series of blends between linear low-density PE and fully-deuterated high-density PE.[7] These blends show almost perfect cocrystallization behavior at any blend ratio and were useful for the investigation of aggregation state of PE chains in the crystal lattice.[7]

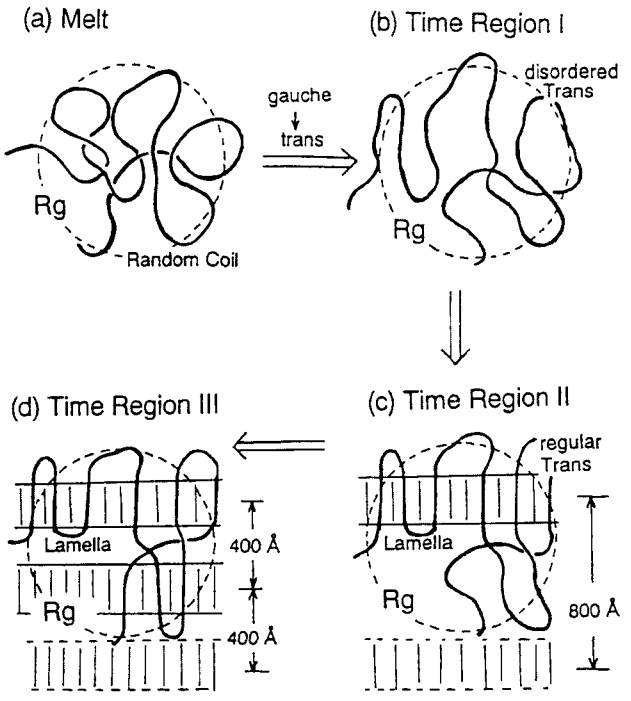

Figure 4. An illustration of structural evolution in the isothermal crystallization of PE (quoted from S. Sasaki, K. Tashiro, N. Gose, K. Imanishi, M. Izuchi, M. Kobayashi, M. Imai, M. Ohashi, Y. Yamaguchi, and K. Ohyama, *Polym. J.*, **31**, 677 (1999)).

Isothermal Crystallization of Polyoxymethylene. A study of isothermal crystallization process of polyoxymethylene (POM) is difficult because of the easy thermal decomposition at high temperature and rapid crystallization rate. Then we used a POM sample including small amount of ethylene oxide as comonomer component to avoid these problems without lost of any essential features of crystallization behavior of POM homopolymer. Another important idea in the crystallization study of POM is a utilization of characteristic infrared spectral data. Depending on the external shape or the morphology of crystalline phase, the infrared bands of A_2 symmetry species shift the peak positions remarkably.[8,9] In fact, the infrared spectra of POM samples prepared under the various conditions show quite different patterns. The extreme cases are the spectra of the extended chain crystal (ECC) of whisker sample and the folded chain crystal (FCC) prepared from the dilute solution: these two samples show the A_2 bands at the positions different by 100 cm^{-1}. By measuring the infrared spectra during the isothermal crystallization, therefore, we may expect that the change in morphology of the crystallites can be traced concretely. By combining this infrared spectral data with the WAXS and SAXS data, the structural change in the isothermal crystallization process of POM was investigated from the various points of view.[10,11]

Figure 5 shows the infrared spectra of POM measured in the isothermal crystallization process at 130 °C.[11] Because of the complicatedness of infrared spectra, the second-derivatives were calculated and the peak heights were evaluated for the bands intrinsic of ECC and FCC morphologies. As seen in Figure 6, the 1139 cm^{-1} band of FCC morphology started to appear immediately after the temperature jump from the melt. The 902 cm^{-1} band of ECC morphology was observed to appear after 150 sec and increased in intensity. The vibrational frequency of the A_2 band is dependent on the total sum of interactions between transition dipoles included in a crystallite.[9] This sum is determined by the shape of the crystallite or the ratio of radius (R) and height (H) when the crystallite is assumed to be a cylinder, for example.[9] Judging from the position of the observed ECC bands, the ratio R/H was estimated to be about 0.3.

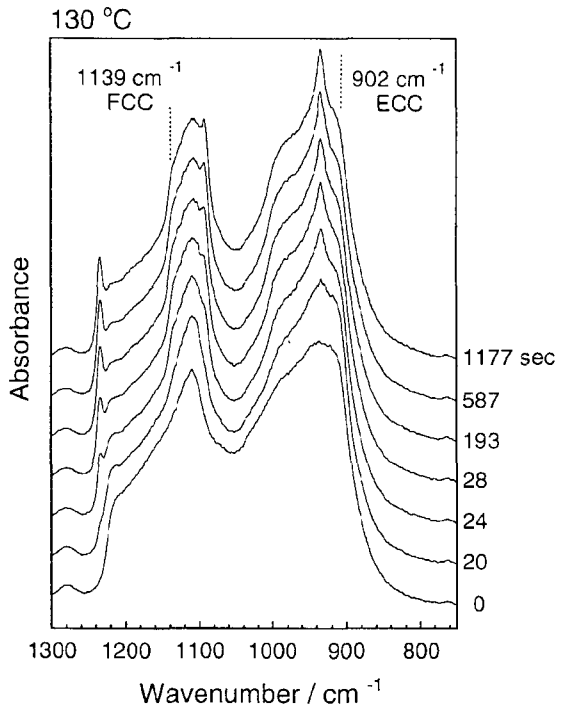

Figure 5. Time dependence of infrared spectra of POM measured in the isothermal crystallization process from the melt.

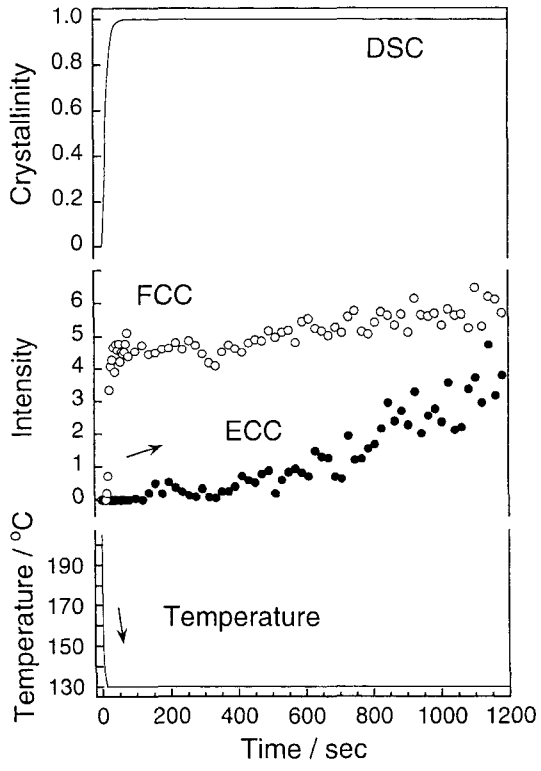

Figure 6. Time dependence of intensity of the infrared bands characteristic of ECC and FCC morphologies evaluated for the isothermal crystallization process of POM from the melt.

The time-resolved SAXS and WAXS measurements were made also at 130 °C. Figure 7 shows the time dependence of SAXS profile. The increment of central peak reflecting a density fluctuation in the melt was difficult to detect clearly, which is a future problem. In the time region of detecting the FCC infrared bands, the SAXS peak (L_1) corresponding to the long period of ca. 140 Å started to appear. After that, this peak decreased in intensity and the peak (L_2) of ca. 70 Å long period increased in stead. In the infrared spectral experiment, the bands intrinsic of ECC morphology were detected at this timing. The generation of stacked lamellar structure of 140 Å and the change to 70 Å are essentially the same phenomena with those observed in the crystallization of PE and can be interpreted in such a way that the amorphous region sandwiched between the original lamellae changes into new crystalline lamella at the secondary crystallization stage. In order to know the details of the crystalline lamellae, the observed SAXS profiles were analyzed on the basis of a theory developed for a stacked lamellar structure model with statistical distribution of lamellar thickness.[12] The detailed description of the data analysis will be reported elsewhere and only the result is shown in Figure 8. The sinusoidal curves shown in the upper part of this figure represent the electron density of lamellae with the thickness distribution taken into account. The simplified illustration of stacked lamellar structure is given below them. The long period changes from ca. 140 to 70 Å. The initially-generated lamellae have a thickness of ca. 70 Å but become thinner with a passage of time, while the newly-generated lamellae increase

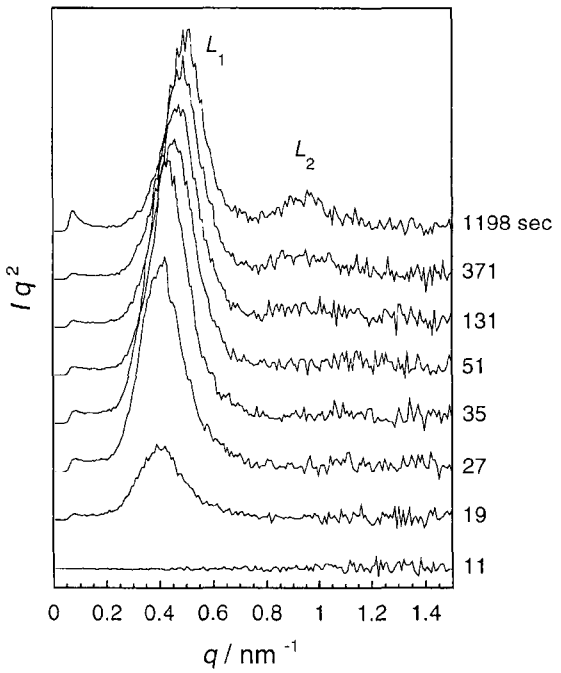

Figure 7. Time dependence of SAXS profile of POM measured in the isothermal crystallization process from the melt.

their thickness from 26 to 33 Å. That is to say, the thickness of these two kinds of lamellae becomes closer to each other, suggesting that the whole system tends to gradually approach the homogeneous lamellar stacking structure.

The timing of secondary crystallization, where the new lamellae appeared in between the originally-stacked lamellae, was found to correspond to the timing of observation of infrared bands intrinsic of ECC morphology. As one possibility the ECC morphology may correspond to the taut tie chains passing through the stacked lamellae. As shown in Figure 9(a), some of the amorphous chain segments have a probability to pass through the neighboring two lamellae.[13,14]

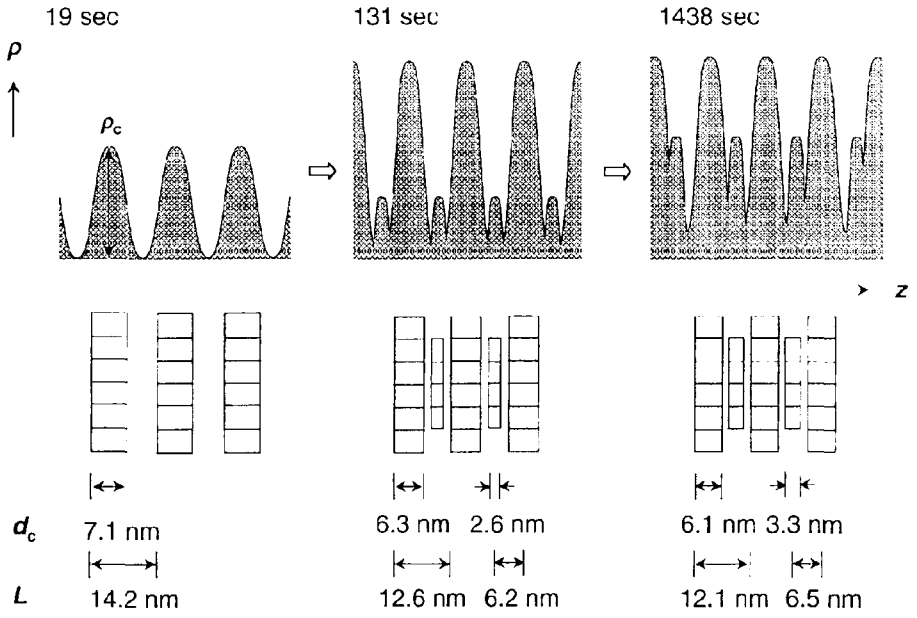

Figure 8. Time dependence of the electron density distribution of POM in the isothermal crystallization process from the melt. The sinusoidal curve with shaded pattern shows an array of lamellae with high electron density, where the Gaussian distribution of the lamellar thickness was taken into account.

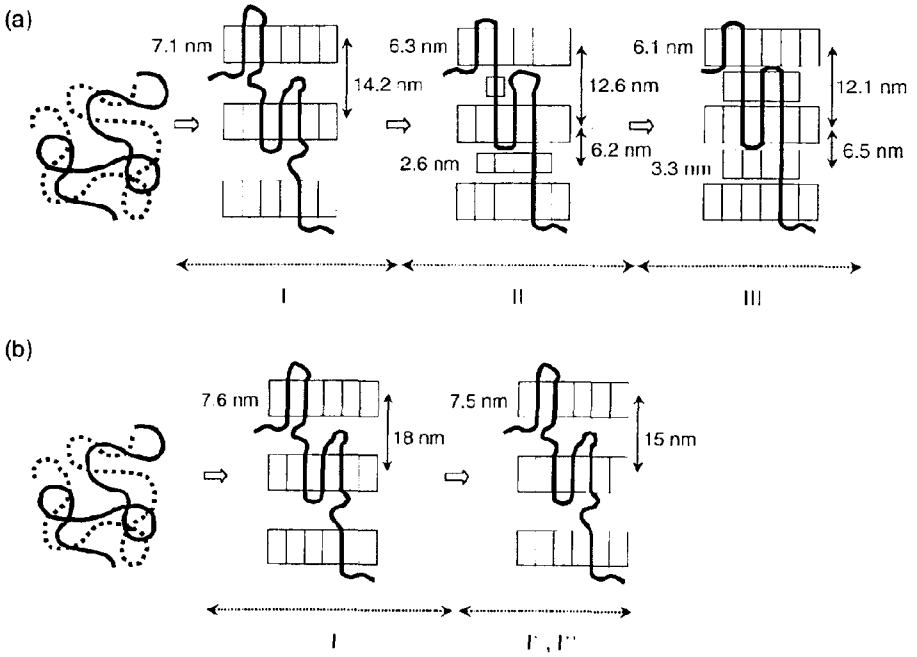

Figure 9. Illustrations of structural evolution in the isothermal crystallization of POM at (a) 130 °C and (b) 150 °C.

When this amorphous region regularizes into a new lamella, the amorphous chain segment changes into straight stem and the total length of the extended segment is about 200 Å in case of Figure 9(a). As mentioned above, from the peak position of the ECC infrared bands, the *R*/*H* ratio of a cylinder, where the dipoles interact coherently, is estimated to be about 0.3, giving an image of ECC region with $R = 60$ Å and $H = 200$ Å. That is to say, these taut tie chains are speculated to form a small bundle passing through the neighboring lamellae. Because this bundle is small, it should melt at much lower temperature than the melting point (ca. 190 °C) of whisker sample consisting of almost infinitely long chains. In fact, the infrared bands observed in the crystallization process were found to disappear already around 135 °C in the reheating process from room temperature.

When the crystallization experiment was carried out at 150 °C, the formation of stacked lamellae with long period of ca. 150 Å was detected in the SAXS measurement, but the secondary crystallization and the corresponding change in the long period were not detected in the measurement time range. Correspondingly the infrared bands of ECC morphology were not detected at 150 °C. The structural evolution at 150 °C is given in Figure 9(b).

Isothermal Crystallization and Ferroelectric Phase Transition of VDF-TrFE Copolymer. VDF-TrFE copolymers show the ferroelectric phase transition between nonpolar high-temperature (HT) phase and polar low-temperature (LT) phase at a Curie transition temperature (T_c), where the remarkable changes in physical properties are observed.[15] As shown in Figure 10, the molecular chains in the LT phase take the planar-zigzag conformation and are packed together so that the CF_2 dipole moments are parallel to each other along the *b* axis, while in the HT phase the molecular chains take the statistically disordered conformations of TT, TG, TTTG, etc. and rotate violently around the chain axis. It is this large conformational change between trans and gauche forms that causes remarkable changes in packing structure and physical properties.

When the temperature jump is performed from the melt to a temperature region of the HT phase, the crystallization to the HT phase is naturally expected to occur, but the details of the crystallization behavior must be clarified. When the temperature jump is made into a lower temperature region of the LT phase, we may have two possibilities. One is a direct crystallization of the LT phase from the melt. Another one is the two-step transition: the HT phase crystallizes from the melt at first and then it transfers to the LT phase. The HT phase is in a metastable state, and therefore the latter case corresponds to the so-called Ostwald's state rule: even in the transformation from the thermodynamically stable phase A to B, the metastable state C might appear transiently if the metastable state is kinetically more preferable than the energetically stable phase B.[16] In order to check this rule, also, the time-resolved measurement during the isothermal crystallization is needed.

Figure 11 shows the time dependence of WAXS profiles measured for VDF-TrFE copolymer with VDF 73 mol% in the isothermal crystallization process to the HT phase region.[17] The (100) reflection of the HT phase was observed immediately after the jump because of too rapid crystallization rate. The peak position was found to shift gradually toward higher angle side, indicating a contraction of the unit cell size. Besides the half width decreased in parallel. These observations indicate that the HT phase in the early stage formed small crystallites in which the molecular chains were loosely packed, but with a passage of time the crystallite size became larger and the chains were more closely packed. Figure 12 shows the time dependence of the X-ray reflection

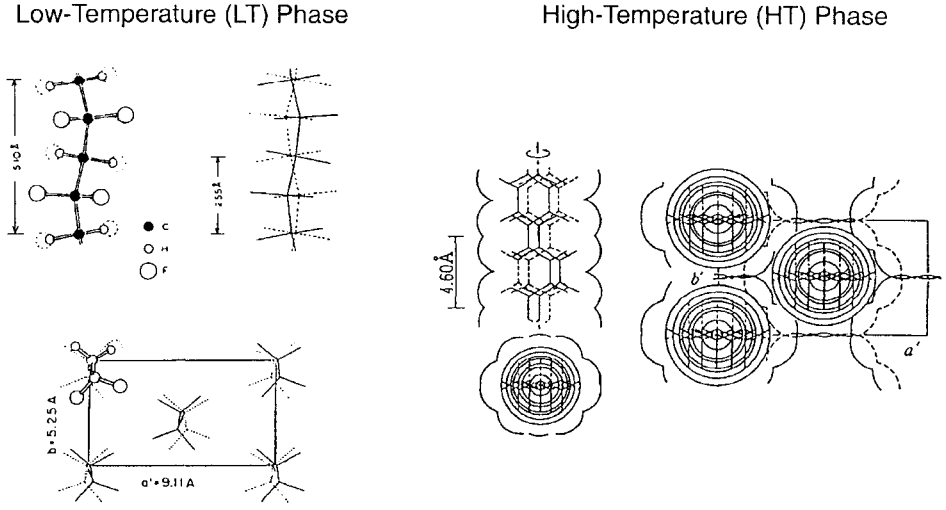

Figure 10. Crystal structures of low-temperature and high-temperature phases of VDF-TrFE copolymer (quoted from K. Tashiro, *Ferroelectric Polymers: Chemistry, Physics, and Technology*, H. S. Nalwa, Ed., p. 63, Marcel Dekker Inc., New York, 1995).

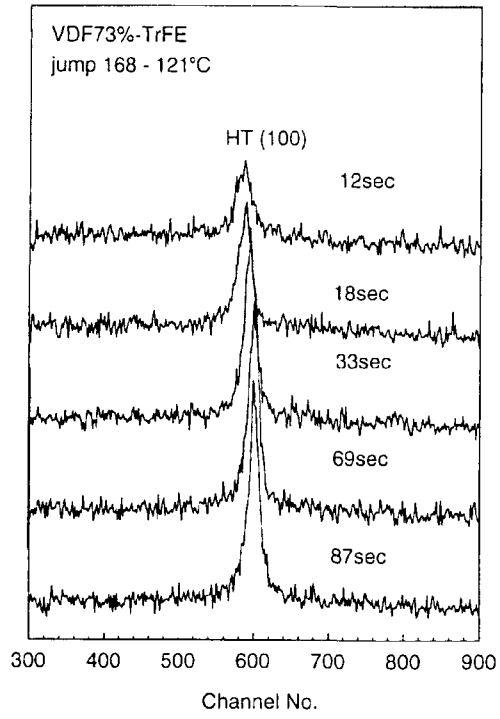

Figure 11. Time dependence of WAXS profile of VDF 73% copolymer measured during the isothermal crystallization from the melt, where the temperature jump was made into the region of the high-temperature phase.

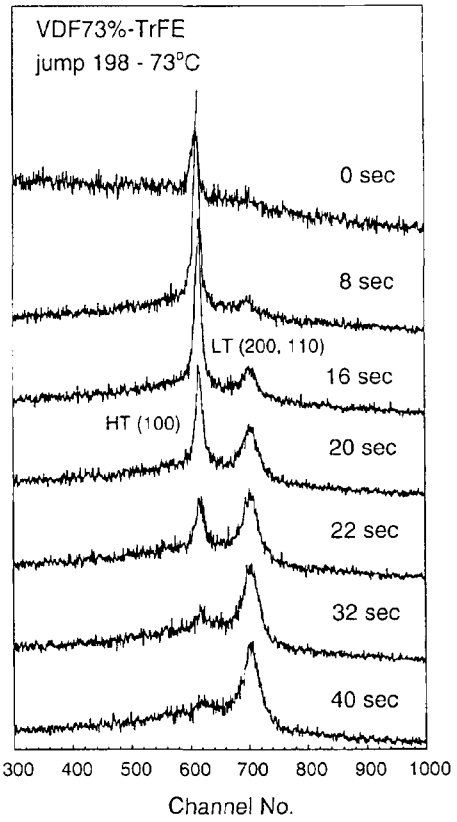

Figure 12. Time dependence of WAXS profile of VDF 73% copolymer measured during the isothermal crystallization from the melt, where the temperature jump was made into the region of coexistence of the high- and low-temperature phases.

profiles measured during the temperature jump into the coexistence region of the HT and LT phases. Immediately after the jump, the HT phase was found to appear rapidly and then decreased in intensity, just when the (200, 110) reflection of the LT phase increased slowly and the HT phase reflection decreased at the same time. As shown in Figure 13 the half width of the HT phase became narrower in a time region of 0-10 sec, similarly to the case shown in Figure 11. The half width of the LT phase reflection was much wider than that of the HT phase. When the transition from the HT phase to the LT phase proceeded furthermore and the fraction of the HT phase was smaller in a later stage of the transition, the half width of the HT reflection became much wider. This is because the remaining HT crystalline part is quite small and is enclosed by the domains of the LT phase.

From the above-mentioned experimental data we may extract the structural change shown in Figure 14. Let us consider the case of Figures 12 and 13 as a typical example. At first the HT phase is crystallized from the melt, but the crystallite size is small and chain packing is loose. As the passage of time the crystallite size becomes larger and the chains are packed more densely. In the HT phase the gauche-type chains are packed in a hexagonal unit cell and rotate violently around the chain axis. Once the conformational change from gauche to trans form occurs, the CF_2 dipoles of

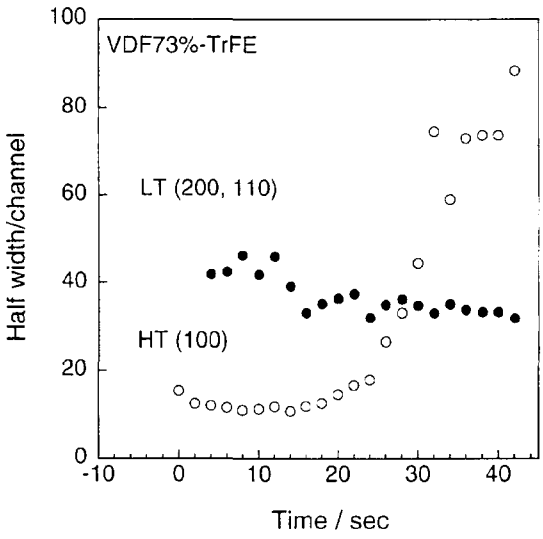

Figure 13. Time dependence of the half-width estimated for the (100) reflection of the high-temperature phase and the (200, 110) reflection of the low-temperature phase in the isothermal crystallization of VDF 73% copolymer from the melt, where the temperature jump was made into the region of coexistence of the high- and low-temperature phases.

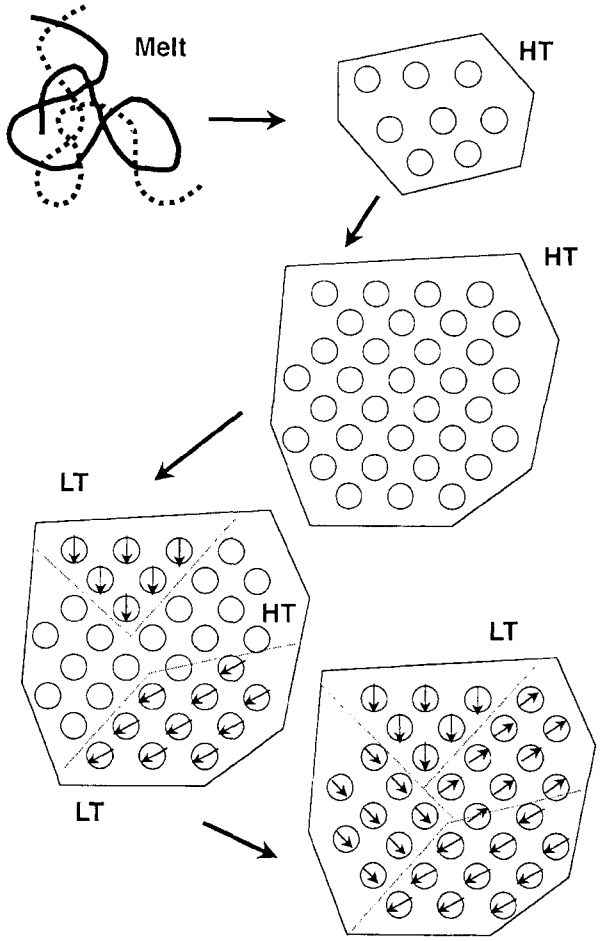

Figure 14. Illustration of structural evolution in the isothermal crystallization and ferroelectric phase transition of VDF 73% copolymer.

the planar-zigzag chains are arrayed along the *b* axis. In this case the polar *b* axis is oriented into one of the six possible directions, each different by 60°. Therefore the parallel array of the CF_2 dipoles gives a small polar domain. As a result the X-ray reflections of the LT phase become broader compared with those of the HT phase.[18] The number of these small domains increases gradually and the whole crystallite consists of an aggregation of domains of different dipole orientations or forms the so-called multi-domain structure.

It should be noticed here that the HT phase reflection was always detected even when the temperature jump was made rapidly from the melt to the temperature region of the LT phase. Kinectics of the crystallization and phase transition processes were analyzed on the basis of Avrami's equation (crystallinity $\propto 1 - \exp[-k \cdot t^n]$). Although the parameters k and n are dependent on the crystallization temperature, the averaged values for the HT phase were $k = 0.01\text{-}0.2$ and $n = 1.6$, while those of the LT phase were $k = 0.0004\text{-}0.002$ and $n = 3$. We may say that the HT phase is kinetically more preferable than the LT phase. Therefore the Ostwald's state rule may be applied to the crystallization of VDF-TrFE copolymer: the thermodynamically-metastable but kinetically- preferable HT phase crystallizes at first and then it transfers to the LT phase more slowly even when the isothermal crystallization is made in the temperature region of the LT phase.

Structural Features Common to Various Polymers. In the present paper the structural evolution process was traced by carrying out the time-resolved measurements of synchrotron-sourced SAXS and WAXS and FTIR spectra for the three cases of isothermal crystallization of PE, POM, and VDF-TrFE copolymer. From all the experimental data collected for these polymers, we may extract some common and characteristic structural features.

In both the cases of PE and VDF-TrFE copolymer, the structurally-disordered metastable state or the hexagonal phase was detected before the appearance of more stable crystalline phase (the orthorhombic phase of PE and the LT phase of VDF-TrFE copolymer). Therefore, it may be said in more general that the crystallization of polymers does not occur directly from the random coils in the melt to the structurally-ordered final crystal phase but proceeds *via* the formation of structurally-disordered (but kinetically-preferable) metastable state, as predicted by the Ostwald's state rule. Such a metastable intermediate state is speculated to generate as a result of density increment in the amorphous state of the melt. The molecular chains in the early stage are loosely packed in small crystallites but grow gradually to more densely packed structure of larger crystallite size. The transition from the intermediate state to the final phase is considered to occur through the disorder-to-order phase transition mechanism. When the structural change is viewed from the scale of lamellar stacking structure on the basis of the SAXS data observed for PE and POM, the long period of the stacked lamellae is found to change from the initially-observed value to the half in the secondary stage of crystallization (800 to 400 Å in PE, and 140 to 70 Å in POM). The amorphous region sandwiched between the stacked lamellae is considered to crystallize to form a new but thin lamella. This heterogeneous structure of stacked lamellae tends to transfer gradually to more homogeneous structure of similar lamellar thickness. From the observation of infrared bands characteristic of ECC morphology in the case of POM, some of the chains are considered to pass through the neighboring lamellae and exist as the taut tie-chain segments at the secondary crystallization stage.

Acknowledgements. The authors wish to thank Exxon Chemicals Inc., Polyplastics Co. Ltd., and Daikin Co, Ltd. for supplying the samples of PE, POM, and VDF-TrFE copolymers, respectively. K. T. acknowledges Dr. Sono Sasaki of Kyushu University for her remarkable contribution in the crystallization study of PE.

References and Notes

(1) Many papers concerning the time-resolved experiments are referred to in the reference: K. Tashiro and S. Sasaki, *Progr. Polym. Sci.*, **28**, 451 (2003).

(2) K. Tashiro, S. Kariyo, A. Nishimori, T. Fujii, S. Saragai, S. Nakamoto, T. Kawaguchi, A. Matsumoto, and O. Rangsiman, *J. Polym. Sci., Polym. Phys.*, **40**, 495 (2002).

(3) K. Tashiro, M. Izuchi, F. Kaneuchi, C. Jin, M. Kobayashi, and R. S. Stein, *Macromolecules*, **27**, 1240 (1994).

(4) K. Tashiro, S. Sasaki, N. Gose, and M. Kobayashi, *Polym. J.*, **6**, 485 (1998).

(5) S. Sasaki, K. Tashiro, M. Kobayashi1, Y. Izumi, and K. Kobayashi, *Polymer*, **40**, 7125 (1999).

(6) K. Tashiro, *KEK Proceedings*, **2001-24**, 5 (2002).

(7) S. Sasaki, K. Tashiro, N. Gose, K. Imanishi, M. Izuchi, M. Kobayashi, M. Imai, M. Ohashi, Y. Yamaguchi, and K. Ohyama, *Polym. J.*, **31**, 677 (1999).

(8) M. Shimomura and M. Iguchi, *Polymer*, **23**, 509 (1982).

(9) M. Kobayashi and M. Sakashita, *J. Chem. Phys.*, **96**, 748 (1992).

(10) H. Hama and K. Tashiro, *Polymer*, **44**, 3107 (2003).

(11) H. Hama and K. Tashiro, *Polymer*, **44**, 2159 (2003).

(12) R. Hosemann and S. N. Bagchi, *Direct Analysis of Diffraction by Matter*, North-Holland, Amsterdam, 1962.

(13) C. M. Guttman and E. A. DiMarzio, *Macromolecules*, **15**, 525 (1982).

(14) S. Balijepalli and G. C. Rutledge, *Comp. Theor. Polym. Sci.*, **10**, 103 (2000).

(15) K. Tashiro, *Ferroelectric Polymers: Chemistry, Physics, and Technology*, H. S. Nalwa, Ed., p.63, Marcel Dekker Inc., New York, 1995.

(16) W. Z. Ostwald, *Physik. Chem.*, **22**, 286 (1987).

(17) K. Tashiro, *Polym. Prepr. Jpn.*, **51**, 449 (2002).

(18) K. Tashiro, R. Tanaka, K. Ushitora, and M. Kobayashi, *Ferroelectrics*, **171**, 145 (1995).